Time-resolved laser-induced fluorescence measurement of ion and neutral dynamics in a Hall thruster during ionization oscillations

Cite as: J. Appl. Phys. **118**, 233301 (2015); https://doi.org/10.1063/1.4937272
Submitted: 31 August 2015 . Accepted: 19 November 2015 . Published Online: 15 December 2015

Andrea Lucca Fabris, Christopher V. Young, and Mark A. Cappelli

Time-resolved laser-induced fluorescence measurement of ion and neutral dynamics in a Hall thruster during ionization oscillations

Andrea Lucca Fabris,[a] Christopher V. Young, and Mark A. Cappelli
Stanford Plasma Physics Laboratory, 452 Escondido Mall, Bldg. 520-118, Stanford, California 94305, USA

(Received 31 August 2015; accepted 19 November 2015; published online 15 December 2015)

The paper presents spatially and temporally resolved laser-induced fluorescence (LIF) measurements of the xenon ion and neutral velocity distribution functions in a 400 W Hall thruster during natural ionization oscillations at 23 kHz, the so-called "breathing mode." Strong fluctuations in measured axial ion velocity throughout the discharge current cycle are observed at five spatial locations and the velocity maxima appear in the low current interval. The spatio-temporal evolution of the ion velocity distribution function suggests a propagating acceleration front undergoing periodic motion between the thruster exit plane and ~1 cm downstream into the plume. The ion LIF signal intensity oscillates almost in phase with the discharge current, while the neutral fluorescence signal appears out of phase, indicating alternating intervals of strong and weak ionization. © *2015 AIP Publishing LLC*. [http://dx.doi.org/10.1063/1.4937272]

I. INTRODUCTION

Hall thrusters[1] exhibit a multitude of coherent and incoherent plasma structures and instabilities when operated under certain conditions.[2] Many are thought to be fundamentally linked to microscopic processes inside the discharge (like electron transport across magnetic field lines and propellant ionization) that in turn affect macroscopic properties like device performance and lifetime. One of the strongest oscillatory regimes is the so-called breathing mode, generated by alternating depletion and re-population cycles of neutrals in the discharge channel determined by the interplay between avalanche ionization and neutral gas transport.[3–5] This regime is characterized by quasi-periodic current oscillations in the 10–50 kHz range, synchronized with the progression and regression phases of the ionization front inside the discharge channel.[3,6]

In order to experimentally probe the fundamental physical processes occurring throughout a discharge breathing oscillation, time-resolved methods able to resolve plasma properties evolving at these time scales are required. Non-intrusive laser-induced fluorescence (LIF) measurements offer a powerful means for obtaining detailed, spatially dependent information about ion and neutral dynamics in plasma systems.[7–9] The velocity of the probed species can be determined from the Doppler shift of the excitation fluorescence spectrum when compared with a stationary reference.

Different techniques have been developed in recent years to accomplish time-resolved LIF measurements in forced or naturally oscillating plasmas. Biloiu *et al.*[10] developed a method to interrogate pulsed plasma sources in argon; Vaudolon *et al.*[11] demonstrated a photon counting technique using a Hall thruster with externally stabilized oscillations; and MacDonald *et al.* demonstrated a sample-and-hold technique[12] to investigate quasi-periodic plasmas, presenting measurements of 3 kHz natural oscillations in a diverging cusped field thruster.[13] The same sample-and-hold architecture was applied by Young *et al.*[14] to capture ion dynamics in an unforced laboratory Hall thruster during 20 kHz natural breathing mode oscillations, and by MacDonald *et al.*[15] to image the evolving ion velocity field in the channel of the commercial Busek BHT-600 Hall thruster oscillating at 50 kHz. Additional time-resolved LIF techniques were developed by Durot *et al.*,[16] demonstrating a transfer function averaging technique applied to a hollow cathode discharge operated with forced current oscillations at 10 kHz, and by Diallo *et al.*,[17] who applied a heterodyne technique based on Fourier decomposition of the periodic LIF signal to a Cylindrical Hall Thruster with forced oscillations at 12 kHz.

In this work, a continuous wave laser-induced fluorescence sample-hold technique provides time-varying ion and neutral velocity data throughout 23 kHz breathing mode oscillations of a Hall thruster operating on xenon in the 400 W power range. This method employs a scanning external cavity diode laser that is amplitude-modulated at a given frequency such that a lock-in amplifier can discriminate the induced fluorescence signal from the bright background emission using homodyne detection. Time-resolved xenon ion velocity measurements on the same thruster were reported in a previous study.[14] This paper presents plasma dynamics recorded at a new thruster operating condition with enhanced time resolution throughout the breathing mode cycle. Measurements are extended to new spatial locations and neutral dynamics are investigated along with the ions to provide additional insight into the overall time-varying characteristics of the thruster plume. Experimental results are discussed in the context of the existing literature on ionization oscillations, with comparisons drawn to previous measurements and numerical simulations.

II. EXPERIMENTAL SETUP

Experiments are conducted in the Stanford Plasma Physics Laboratory vacuum facility. The 4 m long, 1.5 m

[a]Electronic mail: lfandrea@stanford.edu

diameter stainless steel vacuum chamber is equipped with a two-stage cryogenic pumping system: two shrouds cooled with a Polycold Fast Cycle Water Vapor Cryopump (PFC, Model 1100) and two cryopanels cooled with cryogenic helium. The system provides a base pressure of 5×10^{-7} Torr and maintains 5×10^{-5} Torr (uncorrected for xenon) while operating the thruster.

Figure 1 shows a schematic of the Z-70 Hall thruster used in this work. The annular boron nitride channel has an outer diameter of 72 mm, an inner diameter of 42 mm, and a depth of 23 mm, with the channel centerline located at $x =$ 28.5 mm from the main axis. The thruster is operated at an average power of 408 W (240 V anode voltage, 1.7 A anode current) with a xenon mass flow rate of 1.97 mg/s. The external barium oxide IonTech cathode is located 2 cm downstream and 7 cm radially outwards from the thruster main axis, pointing at about 45°, and operates on 150 μg/s of argon. The radial magnetic field strength at the exit plane along the channel centerline is ~160 G. Natural breathing mode oscillations at 23 kHz are observed at these conditions, as shown in Fig. 1. The thruster is mounted on a two-axis horizontal motorized stage for obtaining spatially resolved measurements.

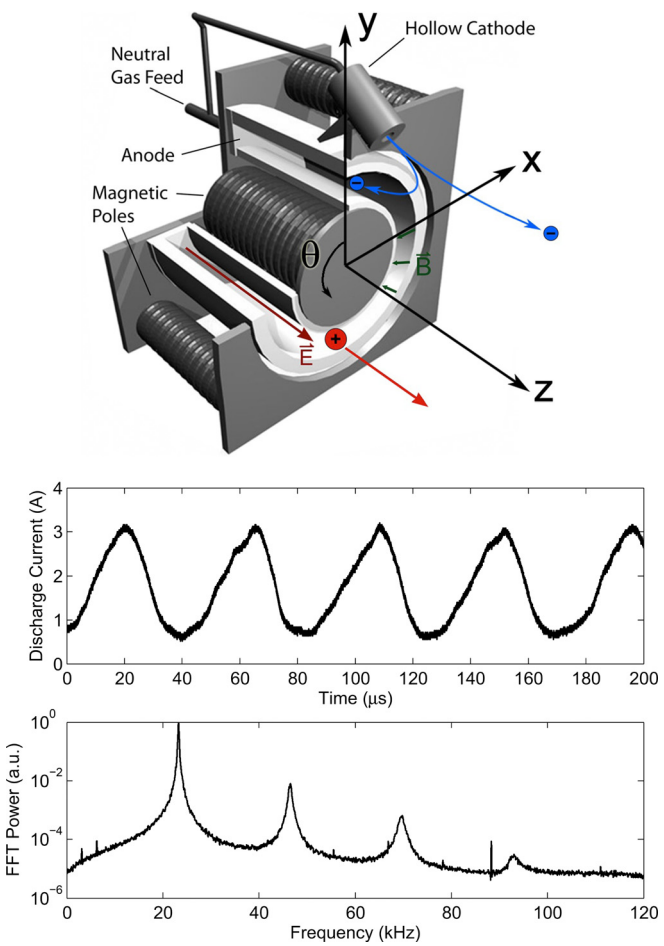

FIG. 1. Schematic of the Z-70 Hall thruster with discharge current trace during operation in the breathing mode regime. An FFT reveals a dominant oscillation frequency of 23 kHz. LIF measurements are taken in the positive x–z plane.

The optical configuration for performing time-synchronized laser-induced fluorescence velocimetry has been described extensively elsewhere,[18] and we summarize the main characteristics here. For measuring ion velocities, the $5d[4]_{7/2} - 6p[3]_{5/2}$ Xe II transition (834.953 nm vacuum) is pumped with ~40 mW of diode laser power and the resulting fluorescence from the $6s[2]_{3/2} - 6p[3]_{5/2}$ transition at 542.1 nm (vacuum) is collected through a Hamamatsu 1P21 photomultiplier tube (PMT) for determining the Doppler shift of the absorption spectrum. The exciting laser beam is generated by a New Focus TA-7600 semiconductor tapered amplifier seeded by a 20 mW tunable external cavity diode laser (New Focus, Model TLB-6817-P) through a polarization-maintaining optical fiber. For studying neutral dynamics, we apply a resonant LIF scheme using the Xe I $6s[3/2]^{\circ}_{2} - 6p[3/2]_{2}$ transition (823.390 nm vacuum) optically pumped by a 13 mW external cavity diode laser (New Focus, Model 6017). The induced fluorescence photons originating from the same transition are collected through a Hamamatsu R3896 PMT.

In both cases, beam diagnostics accurately reconstruct the laser wavelength scan as a function of time. A Fabry-Perot interferometer provides fixed frequency markers (FSR = 1.5 GHz) throughout the scan and a stationary optogalvanic reference signal from the $6p'[3/2]_1 - 8s'[3/2]_1$ Xe I transition (834.973 nm vacuum) is obtained (for ions) from a hollow cathode lamp. This line is spaced 9.03 GHz from the target stationary ion transition. For neutral LIF, the 823.390 nm line provides its own stationary optogalvanic reference. An additional Burleigh WA-1500 wavemeter provides a visual wavelength reading while tuning the laser parameters. The collected light (background emission plus induced fluorescence) is passed through optical shortpass and (10 nm) bandpass filters before PMT detection to reject photons originating from other transitions. A 2 mm mechanical iris reduces the light collection volume and defines the ~1 mm^3 spatial resolution of the measurement.

We track the time evolution of the ion and neutral velocity distribution functions at several points throughout the thruster plume using a sample-and-hold approach. The method relies on generating an acquisition gate locked at a given phase of the oscillating period, in which the PMT signal is sampled, averaged, and held until updating in the following gate one oscillation period later. Using this architecture, only the LIF contribution originating at a given phase of the oscillation is processed during a laser wavelength scan, yielding the ion velocity distribution function (IVDF) representative of the plasma conditions during a short time interval. The overall time evolution of the IVDF is then reconstructed from several scans taken at a variety of phases. In order to reduce campaign time, the PMT signal is split into multiple sample-and-hold branches to simultaneously measure multiple IVDFs during a single laser scan. Two branches were used for the experiments described in this paper.

Acquisition gates are generated with a pulse-delay generator (Stanford Research Systems DG535) triggered by a voltage comparator chip (Model LM339). The latter receives the AC component of the discharge current signal as an input

and produces a positive output for positive values of the discharge current and a null output for negative values. The result is a square wave signal synchronized with the thruster discharge current. The sample-and-hold procedure is implemented through dedicated electronic units satisfying the various requirements of triggering frequency, gate width, and acquisition time for resolving IVDF fluctuations up to 50 kHz. Homodyne detection, implemented by an SRS 850 lock-in amplifier, extracts the weak induced fluorescence signal from the bright spontaneous background plasma emission. The laser beam is amplitude-modulated by a mechanical chopper at a given frequency, f_c, inducing a modulation of the LIF signal at the same frequency. The lock-in amplifier extracts the component of the PMT signal at f_c, which is chosen to be lower than the discharge current fundamental frequency f_0 (typically $f_0/f_c \approx 5$–20) to permit multiple sample-hold updates within a chopping window. Further details regarding this technique, along with applications to dynamic analysis of other types of plasmas such as an AC capillary discharge and a diverging cusped field thruster, may be found in previous work.[12–14,19]

III. RESULTS AND DISCUSSION

A. Time-resolved ion velocity measurements

We track the time-varying ion velocity distribution functions downstream of the exit plane ($z = 0$) at axial positions $z = 5$, 15, and 20 mm along the channel centerline ($x = 28.5$ mm). At $z = 15$ mm, we also move off-axis in either direction, radially inwards to $x = 23.5$ mm and radially outwards to $x = 33.5$ mm. We use a 2 μs acquisition gate spaced in 2–2.5 μs increments throughout the ~43 μs breathing mode oscillation period. Examples of acquisitions taken at $x = 28.5$ mm and $z = 15$ mm are shown in Fig. 2, along with the instantaneous current level corresponding to each time delay (see insets). Each plot reports the normalized LIF signal intensity obtained as a function of laser detuning frequency from the stationary line center. After applying the Doppler shift relation, each trace is representative of the IVDF at a specific instant in time during the oscillation period. Merging these instantaneous profiles reconstructs the overall time evolution of the IVDF throughout the breathing mode oscillation at the various interrogated points.

Figure 3 illustrates the time-dependent IVDFs at the probed spatial locations. Each fluorescence trace $S(t_n, v)$, taken at a given instant t_n, is weighted by the total integrated scan intensity, yielding: $I(t_n, v) = S(t_n, v) / \int_{v_{min}}^{v_{max}} S(t_n, v)\, dv$. Then, each contour plot is normalized by the overall maximum value: $I(t, v)/I(t, v)_{max}$. This normalization is chosen to highlight the evolving structures in velocity space despite strong signal attenuation experienced in the current trough ($t = 20$–40 μs). A higher intensity color (red, pink) represents narrow and intense features in velocity space, while lower intensity colors denote velocity classes with a lower fractional weight and usually indicate ion velocities distributed over a broader velocity range.

The time-resolved IVDF results are also presented in Fig. 4, visualized in a complementary way. Here, each IVDF set, associated with one nominal 23 kHz representation of the quasi-periodic thruster discharge current (the term "quasi" acknowledges the small period-to-period frequency drift about the fundamental evident in the FFT of Fig. 1), is repeated four times in post-processing to illustrate the oscillatory characteristics of breathing mode operation. In these plots, the color scale represents the true LIF signal intensity, proportional to the probed excited state densities of the various ion velocity classes present at a given spatial location and instant in time. The integral average of these LIF profiles over the current cycle recovers the more commonly measured time-averaged IVDF traces.[7,8] For each probed spatial point, we have verified that the integrated time-resolved measurements adequately reproduce time-averaged traces obtained directly from standard LIF measurements without sample-hold processing. An example from the point at $x = 28.5$ mm, $z = 5$ mm, is shown in Fig. 5(a). Features present in the time-averaged signal may be traced to multiple dominant ion velocity populations appearing during certain phases of the discharge current, as illustrated in Fig. 5(b).

Strong variation in ion velocity is observed over the oscillation period at each spatial point. All of the interrogated locations show a higher ion velocity in the current trough ($t = 20$–40 μs) between consecutive discharge current peaks. The velocities attain their lowest values during the ramp up in discharge current, after which ions are accelerated to near their maximum velocities as the current ramps down. At $z = 5$ mm, the velocity doubles from 7.5 km/s to 15.4 km/s, indicating strong variations in the local accelerating potential structure over the breathing mode cycle. This behavior is also observed downstream, where velocities at $z = 15$ mm and $z = 20$ mm fluctuate up to 38% and 34%, respectively, about their median values.

Similar trends were observed by Bouchoule *et al.*[20] when probing transient phenomena in an SPT-100 Hall thruster oscillating with a ~35–40 μs period at 400 V anode potential. Time-variation of the ion beam energy at the exit plane was determined by placing a retarding field energy analyzer (RFEA) 0.8 m downstream and correcting for time-of-flight effects. The measurements revealed ion energies ranging from 310 to 380 eV, with the energy minimum occurring at high instantaneous values of the discharge current. These observations are in agreement with our spatially and temporally resolved LIF measurements, which are capable of probing directly inside the acceleration region without perturbing the plasma discharge.

As expected, axial ion acceleration is observed moving downstream of the thruster exit plane. The increase in velocity between $z = 5$ mm and $z = 15$ mm demonstrates that the acceleration front extends (at least for some time) beyond the thruster channel (another characteristic in common with the SPT-100).[20] The acceleration in this region is most pronounced in the interval of increasing discharge current, when most probable ion velocities increase from 8 km/s to 12 km/s over 10 mm. This indicates that the accelerating potential drop is near its maximum expansion into the near field plume. After the discharge current peak, additional ion acceleration between $z = 5$ mm and $z = 20$ mm is minimal, indicating the bulk of the acceleration front has moved upstream towards the exit plane region. Ions slow substantially at

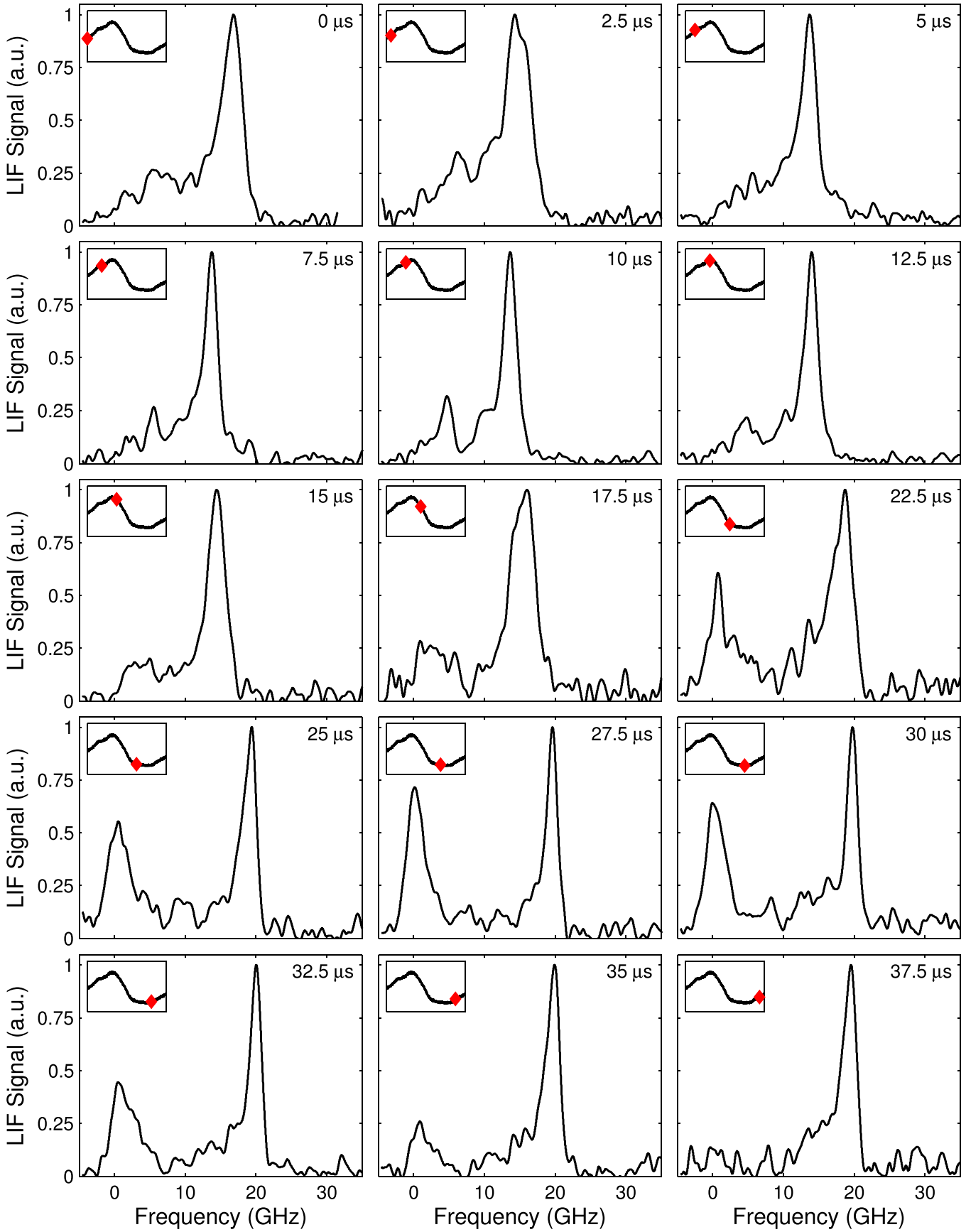

FIG. 2. Time-resolved normalized xenon ion LIF traces as a function of laser detuning frequency from stationary line center acquired $z = 15$ mm downstream of the exit plane, at the point along the channel centerline ($x = 28.5$ mm). The profiles highlight the presence of a slower ion population, in addition to the main accelerated one, which becomes prominent in the latter half of the oscillation cycle. The insets represent the discharge current cycle, with the corresponding current level at each time point indicated by the marker (◆).

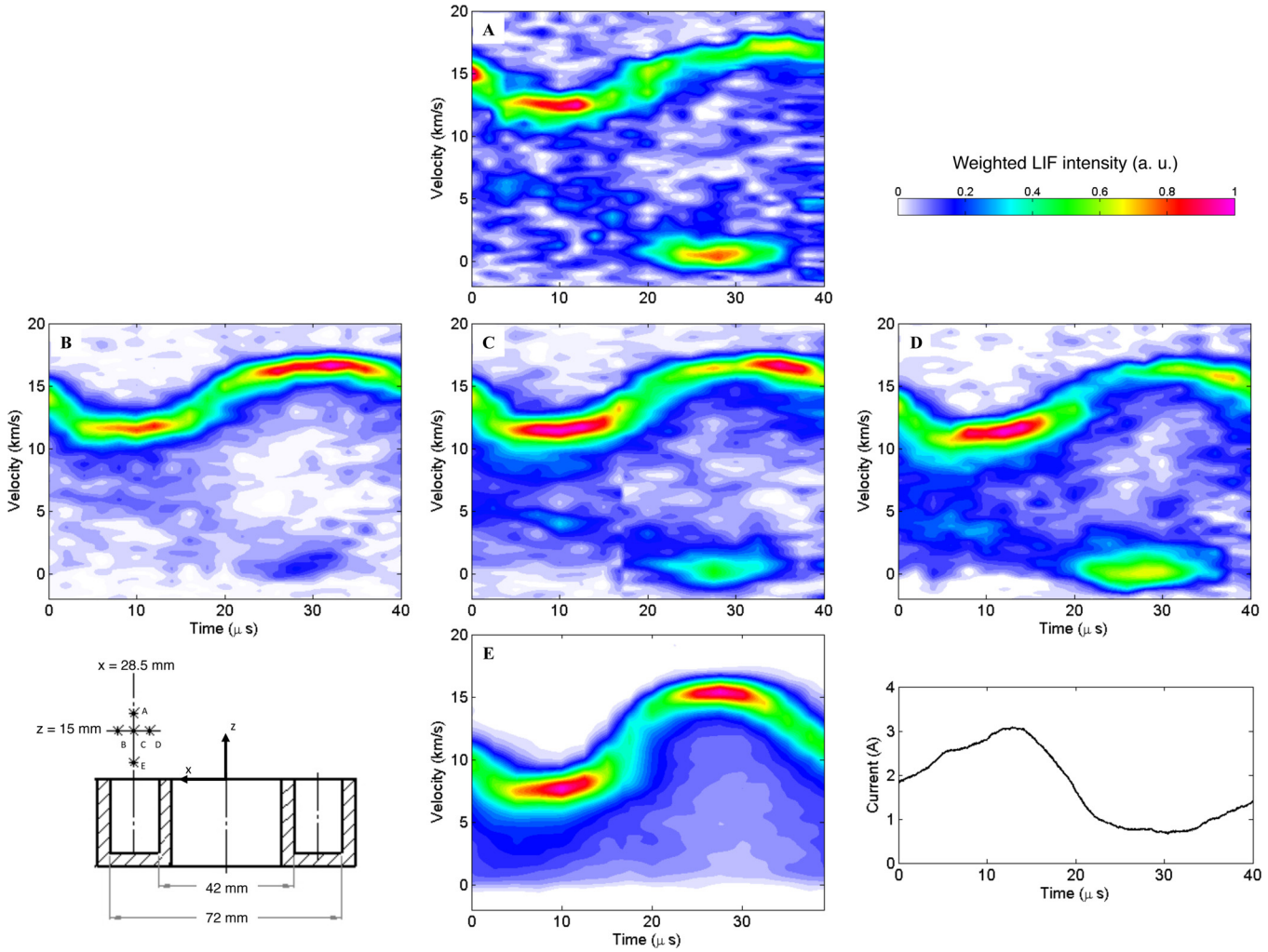

FIG. 3. Contour maps of the acquired lineshapes for xenon ions; a single laser scan like those shown in Fig. 2 constitutes a vertical strip at a given time delay. Each trace is normalized by the total intensity of the scan to show structure despite variations in signal intensity with time. A higher intensity color (red, pink) is representative of narrow and intense features in velocity space, while lower intensity colors indicate velocity classes of lower fractional weight (for example, during time frames in which ions spread over a broader velocity range).

$z = 5$ mm as the current builds out of the trough, presumably due to the main potential gradient extending outside again.

A similar process was observed in two-dimensional (radial-axial) hybrid particle-in-cell (PIC) simulations by Bareilles *et al.*[21] Using PIC ions and fluid electrons, the authors studied the effects of ionization and transit-time oscillations on the operation of a Hall thruster (similar to the SPT-100) at various operating conditions. We show good agreement between the present experimental results and the physical description of ionization oscillations offered by the hybrid PIC simulations. During the upward ramp of the discharge current, the ionization rate is maximum in the peak magnetic field region and most of the ion acceleration front extends outside the thruster. At the discharge current peak, the ionization rate is maximized and the ionization zone spreads over a larger volume of the discharge channel, strongly depleting the neutral population. The following phase is characterized by decreasing discharge current, minimum neutral density, and higher electric field, with the main acceleration region located near the thruster exit plane. The neutral density then increases, beginning a new cycle. All these characteristics are consistent with the measurements presented here and the discussion above. The hybrid simulations also capture a periodic change of the ion beam divergence during these ionization oscillations, characterized by a larger divergence angle when the acceleration zone extends into the near field. This has been observed experimentally using CCD imaging,[22] and planned time-resolved LIF measurements of the radial ion velocity components, in addition to the axial ones, will experimentally verify this process is occurring in the Z-70.

By $z = 15$ mm, the ion acceleration is almost fully developed throughout the entire cycle, with only a small additional increase in velocity occurring downstream at $z = 20$ mm. Measured profiles of the primary accelerated ion population do not significantly differ between the three radial points investigated at $z = 15$ mm (see Figs. 3 and 4). However, interesting differences in the IVDFs arise at low velocities: slower secondary ion populations appear over certain time intervals, becoming more pronounced towards the thruster main axis (see panels at $x = 23.5$ mm) and weakening away from the axis ($x = 33.5$ mm). A $\sim$4 km/s population is apparent just

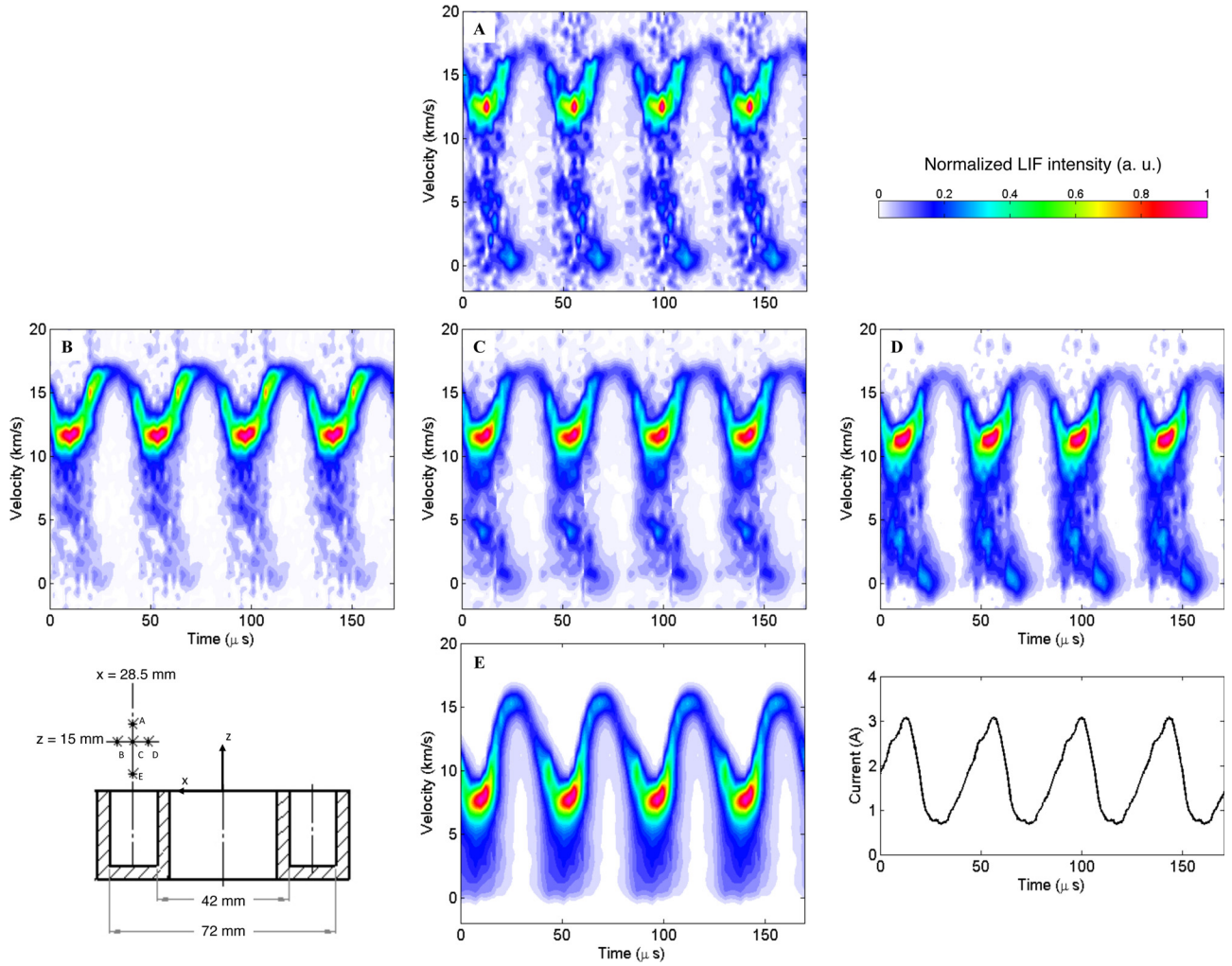

FIG. 4. Contour maps of the acquired LIF lineshapes for xenon ions, repeated over four typical 23 kHz discharge current cycles. The color scale represents true fluorescence signal intensity, proportional to the probed excited state density for a given ion velocity class, normalized by the maximum value in each panel.

before the current peak, while a slower class of ions in the 0–2 km/s range forms in the current trough. As evidenced in the individual traces of Fig. 2 (at $z = 15$ mm along the channel centerline), the lowest velocity ions produce a fluorescence intensity comparable to that of the main accelerated population between 22.5 and 35 μs. At this location, the 4 km/s population is less pronounced in comparison. The relative intensity of the lowest velocity structure increases further downstream at $z = 20$ mm, where it temporarily overtakes that of the main accelerated population (Fig. 3).

The origin of this low velocity ion class is tied to temporally and spatially dependent physical processes in the thruster. Low ion velocity populations have appeared previously in time-averaged[23,24] and time-resolved[14,25] LIF measurements of Hall thruster plumes and different hypotheses explaining their presence have been suggested, including residual ionization beyond the channel, charge-exchange collisions with neutrals, and geometrical effects attributed to a divergent plume originating from elsewhere in the annular channel. External ionization remains a possible option, and additional studies are needed to justify the spatial and temporal dependence of the feature. The possibility of charge-exchange collisions is investigated in Sec. III B, seeking evidence of correspondingly high velocity neutrals using the same time-resolved LIF approach. Geometrical effects would imply a very large divergence angle (~70°–72°) for a short period of time, but primarily radially directed ions leaving the center of the channel on the opposite side at 15 km/s would arrive at the measurement locations ~3.5 μs later, within the time frame to be recorded here as a low axial velocity population of ions. The observed axial velocities of the 0–2 km/s population are too slow to traverse 15–20 mm downstream in this amount of time; however, a fact that may point towards alternate explanations instead.

Another noteworthy characteristic of the IVDF traces is how the broadening of the main feature changes during the different phases of the ionization oscillations. A wider distribution of velocities is observed during the high current interval, when the ionization rate is higher and the accelerating potential drop extends into the near field plume. This creates a smattering of newborn ions throughout velocity space that have sampled differing amounts of the potential drop based on its spatial-temporal history and the precise location and moment of the ionization event. This broadening is

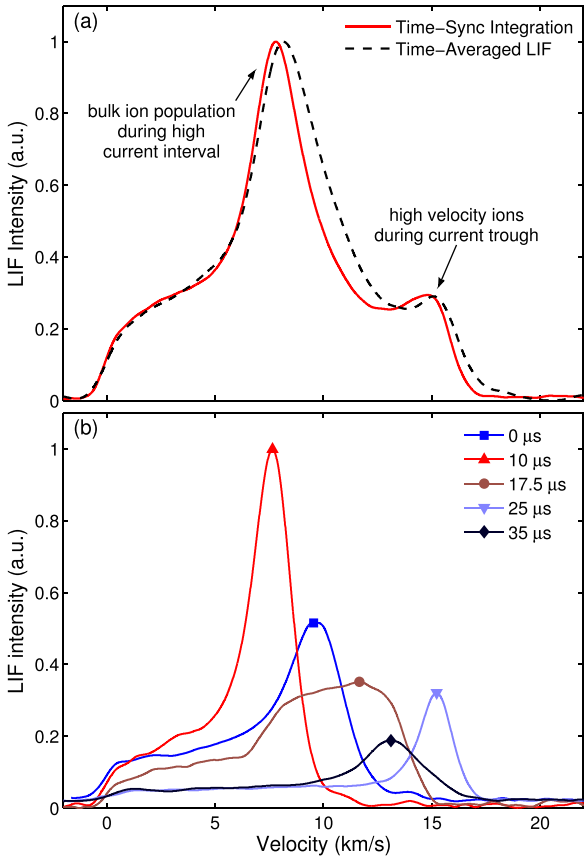

FIG. 5. (a) Comparison between xenon ion time-averaged excitation fluorescence spectra derived from the integration of time-resolved LIF measurements (solid line) and direct measurements bypassing the sample-hold circuits (dashed line) at $x = 28.5$ mm, $z = 5$ mm. (b) Examples of xenon ion time-resolved LIF profiles (normalized by the overall maximum) obtained at different phases of the discharge current cycle at $x = 28.5$ mm, $z = 5$ mm. Multiple ion velocity populations dominate at different times throughout the current period, combining to generate the overall time-averaged profile.

particularly visible at $z = 5$ mm in Fig. 4. Later, as the current dips, the acceleration front moves back upstream, the ionization rate decreases and becomes more localized, ions traverse the acceleration zone much more uniformly, and the IVDF structure becomes consequently narrower.

The fluorescence intensity traces illustrated in Fig. 4 are indicative of the evolving local probed excited state ion density of a given velocity class. The peak LIF signal intensity follows the general shape of the current trace. First, fluorescence signal increases during the ramp up in discharge current as the rate and spatial extent of ionization increases the population of ions and electrons. LIF signal intensity peaks around the current maximum, and falls off substantially in the current trough. This behavior is consistent with previous spectroscopic measurements of time-varying excited-state ion distributions within a Hall thruster channel[11,22,26] and the physical analysis of breathing mode dynamics offered above and elsewhere in the literature.[4,6] Note that the LIF signal intensity is proportional to the metastable ion density, while numerical analyses usually report the global ion density. A complete collisional-radiative model, including higher excited states, would be required in order to give a complete picture of the excited state population dynamics and, in particular, fully resolve the relationship between ground and metastable ion densities.

Finally, we verify that integrating the acquired time-resolved LIF profiles over time recovers the time-averaged IVDF obtained by the standard LIF technique without sample-and-hold processing. These traces for the point $z = 5$ mm, $x = 28.5$ mm are shown in Fig. 5(a) as an example. Here, the most probable (peak) average ion velocity is found to be $\sim$8 km/s, which is closer to the lower bound of the observed time-dependent velocity fluctuations at this location (Fig. 3). The origin of this effect is explained in Fig. 5: since the observed time-averaged LIF trace is derived from time-resolved IVDFs weighted by intensity, lower velocity ions present in the brighter high current interval contribute more to the integral. The less intense, higher velocity ions appearing later in the current trough form the bump observed near 15 km/s in Fig. 5(a). This analysis highlights how only partial information about global ion dynamics may be extracted from the time-averaged IVDF, since it does not discriminate between ion velocity classes present over the entire cycle and those emerging only as transients. Additionally, the time-averaged analysis cannot distinguish broadening of the overall lineshape due to time-dependent oscillations of a narrower distribution (as is the case here) from other mechanisms. Such details can only be extracted using time-resolved measurements.

B. Time-resolved neutral velocity measurements

This section describes time-resolved measurements of the neutral velocity distribution function in the Hall thruster plume. The operating conditions are identical to those used previously with ions. We interrogate two different spatial points along the channel centerline ($x = 28.5$ mm): one at the exit plane, $z = 0$ mm, and one downstream at $z = 15$ mm. Time-resolved measurements of the ion velocity distribution function at the latter point (Fig. 4) show the appearance of well-defined low velocity structures; the presence of a correspondingly high velocity neutral population would then point towards charge-exchange collisions.

The structure of the probed 823.2 nm line is complex due to the presence of multiple hyperfine transitions. Determining the full set of fluid quantities (such as temperature or mean velocity) would require lineshape modeling methods that account for the hyperfine structure, Zeeman splitting, and other broadening mechanisms.[27] For the physical discussion that follows, we use quantities that are unaffected by lineshape broadening: most probable velocity and peak LIF intensity. These two properties are obtained via the Doppler shift and peak value, respectively, of the structure at line center of the raw LIF profiles.

The contour plot in Fig. 6(b) shows the neutral velocity time history at the thruster exit plane during a discharge current cycle. We measure a time-averaged peak velocity of $\sim$350 m/s, a value in agreement with previous measurements on similar Hall discharges.[7,8,28] The velocity profiles at this location do not seem to change appreciably over time. An interesting feature is observed in the excitation fluorescence intensity profile (which also appears in Fig. 7), in which the

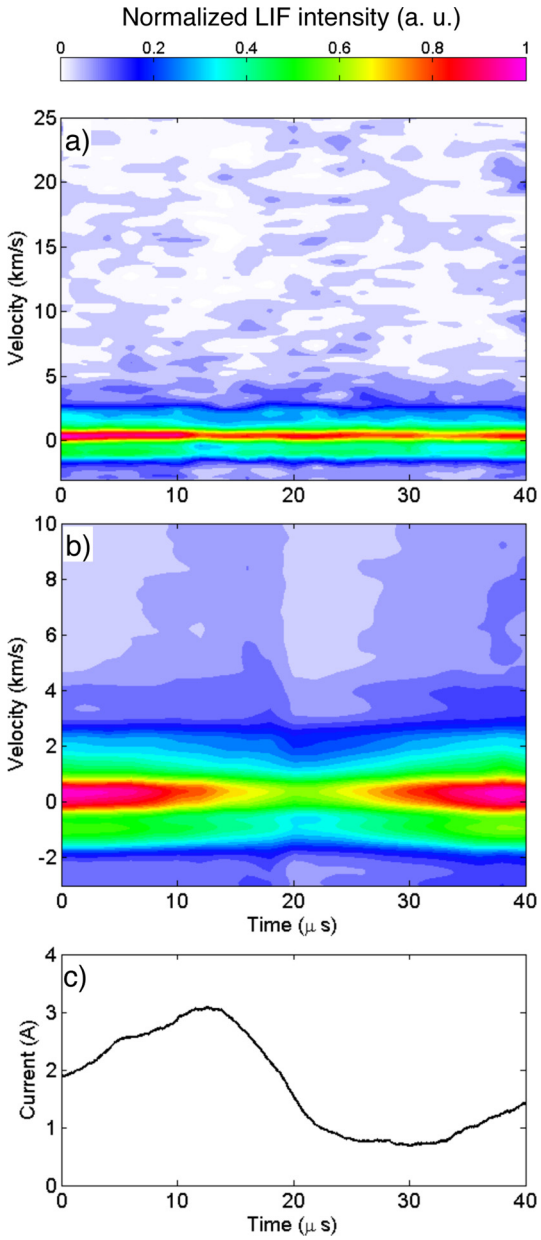

FIG. 6. Contour maps of measured xenon neutral fluorescence lineshapes at (a) $z = 15$ mm, and (b) the exit plane ($z = 0$), along the channel centerline. A single laser scan forms a vertical strip at a given time delay. The color scale represents the true LIF signal intensity normalized by the maximum value in each panel. (c) Discharge current trace for reference.

intensity fluctuation leads that of the current by about a quarter oscillation period (90° phase lead). The LIF intensity peaks about 12 μs before the current maximum, while the current is still ramping up. As mentioned above, the fluorescence signal intensity is representative of the lower state density of the probed transition, the time evolution of which results from a combination of several processes including electron impact ionization and excitation, radiative decay, and local electron and ion transport mechanisms. These various processes interact in complex ways, but a possible reason behind the observed decrease in fluorescence intensity when the discharge current peaks is the increase in propellant ionization associated with this phase of the breathing mode cycle. During this period, the probed metastable neutral

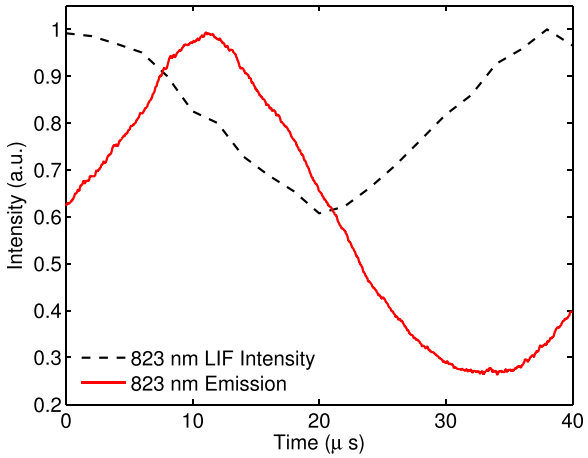

FIG. 7. Normalized peak LIF signal intensity at the exit plane ($z = 0$), in addition to spontaneous plasma emission intensity at 823 nm detected by the PMT. The LIF signal intensity leads the discharge current by a quarter cycle (90°), showing a possible depopulation of the probed excited state due to excitation to upper energy levels and ionization while the current is high. In contrast, the spontaneous emission intensity at 823 nm appears in phase with the discharge current oscillation.

population could be depleted by increased excitation to upper states and ionization.

This hypothesis is supported by the emission data shown in Fig. 7, collected with a photomultiplier tube from the same 823 nm transition (recall that a resonant LIF scheme is used for neutrals). Processing the PMT signal through a lock-in amplifier discriminates laser-induced fluorescence photons from the overall background emission, yielding information about the lower state density in the localized LIF measurement volume. The raw PMT signal, however, primarily contains data from the bright plasma background emission, providing information about the upper state population (over the entire optical collection path). As shown in Fig. 7, the total emission intensity closely tracks the current profile. We also know that metastable ion density increases along with the current from Fig. 4, together indicating an energy flow towards higher xenon neutral excited states and the continuum (ionization) when the current is high. This view is supported by the observed corresponding decrease in lower probed neutral state population density during this time.

Figure 6(a) shows the time-dependent neutral velocity over a discharge current cycle at $z = 15$ mm downstream of the exit plane along the channel centerline. The measured time-averaged neutral velocity is ~400 m/s, and again we do not see any significant evolution of the velocity profile throughout the breathing mode cycle. The fluorescence intensity also does not show any distinct behavior, with only a slight decrease observed moving from the high current to low current interval. This point is investigated mainly for evidence of fast neutral atoms that would be produced by charge-exchange collisions with accelerated ions. The LIF spectrum for velocities above 2 km/s does not show any signs of additional populations, and consequently we cannot report any evidence for charge-exchange in this study.

If the presence of fast neutrals would demonstrate charge-exchange processes, their absence cannot completely exclude charge-exchange as a possible mechanism behind

the observed low ion velocity population, since the signal intensity originating from the presumed high neutral velocity population may be significantly weaker than the baseline neutral signal. The resonant neutral LIF scheme used in this study is much stronger than that used for ions, and it is possible that strong background emission, persisting even through the current trough, overshadows the signal originating from any additional low density populations. Moreover, the absence of fast neutrals in this specific probed metastable state does not directly imply their absence at the ground or other excited levels.

IV. CONCLUSION

This paper reports time-resolved continuous wave laser-induced fluorescence measurements of a 400 W Hall thruster operating on xenon, during 23 kHz breathing mode oscillations. Time varying ion and neutral velocity distribution functions are obtained in the near-field plume throughout the discharge current cycle. Time series taken at several spatial points along the channel centerline show ion acceleration through a fluctuating potential drop located (at least for some times) downstream of the exit plane. Variations in measured axial ion velocity throughout the discharge current cycle are observed at each location, with the maxima appearing in the low current interval. Excitation fluorescence intensity signal (proportional to the probed lower excited state ion density) is greatest during the upward ramp in discharge current, peaks around the current maximum, and falls off substantially in the trough between current peaks.

The appearance of low ion velocity structures into the plume is further investigated with time-synchronized LIF of excited xenon neutrals, seeking evidence of charge-exchange collisions. Neutral measurements do not show any such evidence at this time, although we cannot completely exclude this hypothesis from a null result probing a supposed weak population in just one metastable state. Finally, time-resolved LIF measurements on xenon neutrals show that the probed excited neutral population at the exit plane populates and depopulates 90° out of phase with the discharge current. Experimental evidence suggests this effect is associated with stronger excitation to higher energy states and ionization during the high current period.

Future work will involve further analysis of excited neutral dynamics within the thruster channel and improving the spatial resolution of the time-resolved ion velocity measurements to capture the time-dependent ion acceleration front. Radial ion LIF measurements will complete the physical picture of the dynamic near-field plume region, showing how the 2-d ion velocity vectors (and consequently, the plume divergence angle) change with time throughout the breathing mode cycle.

ACKNOWLEDGMENTS

This work was sponsored by the U.S. Air Force Office of Scientific Research with Dr. M. Birkan as program manager. C.Y. acknowledges support from the DOE NSSA Stewardship Science Graduate Fellowship under Contract No. DE-FC52-08NA28752 and the Stanford Graduate Fellowship.

[1]M. Cappelli, Phys. Today **62**(4), 76 (2009).
[2]E. Choueiri, Phys. Plasmas **8**, 1411 (2001).
[3]S. Barral and Z. Peradzyński, Phys. Plasmas **17**, 014505 (2010).
[4]J.-P. Boeuf and L. Garrigues, J. Appl. Phys. **84**, 3541 (1998).
[5]F. Darnon, L. Garrigues, J. Boeuf, A. Bouchoule, and M. Lyszyk, IEEE Trans. Plasma Sci. **27**, 98 (1999).
[6]S. Barral and E. Ahedo, Phys. Rev. E **79**, 046401 (2009).
[7]R. Cedolin, W. Hargus, Jr., P. Storm, R. Hanson, and M. Cappelli, Appl. Phys. B **65**, 459 (1997).
[8]W. Hargus, Jr. and M. Cappelli, Appl. Phys. B **72**, 961 (2001).
[9]S. Mazouffre, Plasma Sources Sci. Technol. **22**, 013001 (2013).
[10]I. A. Biloiu, X. Sun, and E. E. Scime, Rev. Sci. Instrum. **77**, 10F301 (2006).
[11]J. Vaudolon, L. Balika, and S. Mazouffre, Rev. Sci. Instrum. **84**, 073512 (2013).
[12]N. MacDonald, M. Cappelli, and W. Hargus, Jr., Rev. Sci. Instrum. **83**, 113506 (2012).
[13]N. MacDonald, M. Cappelli, and W. Hargus, Jr., J. Phys. D: Appl. Phys. **47**, 115204 (2014).
[14]C. V. Young, A. Lucca Fabris, and M. A. Cappelli, Appl. Phys. Lett. **106**, 044102 (2015).
[15]N. MacDonald-Tenenbaum, C. V. Young, A. Lucca Fabris, M. Nakles, W. A. Hargus, Jr., and M. A. Cappelli, in *Proceedings of the 34th International Electric Propulsion Conference* (Hyogo-Kobe, Japan, 2015), IEPC-2015-350.
[16]C. Durot, A. Gallimore, and T. Smith, Rev. Sci. Instrum. **85**, 013508 (2014).
[17]A. Diallo, S. Keller, Y. Shi, Y. Raitses, and S. Mazouffre, Rev. Sci. Instrum. **86**, 033506 (2015).
[18]A. Lucca Fabris, C. V. Young, M. Manente, D. Pavarin, and M. A. Cappelli, IEEE Trans. Plasma Sci. **43**, 54 (2015).
[19]A. Lucca Fabris, C. V. Young, and M. A. Cappelli, Plasma Sources Sci. Technol. **24**, 055013 (2015).
[20]A. Bouchoule, C. Philippe-Kadlec, M. Prioul, F. Darnon, M. Lyszyk, L. Magne, D. Pagnon, S. Roche, M. Touzeau, S. Béchu *et al.*, Plasma Sources Sci. Technol. **10**, 364 (2001).
[21]J. Bareilles, G. Hagelaar, L. Garrigues, C. Boniface, J. Boeuf, and N. Gascon, Phys. Plasmas **11**, 3035 (2004).
[22]D. Pagnon, F. Darnon, S. Roche, S. Bechu, L. Magne, A. Bouchoule, M. Touzeau, and P. Lasgorceix, AIAA Paper No. 99-2428 (1999).
[23]W. A. Hargus, Jr. and C. S. Charles, J. Propulsion Power **26**, 135 (2010).
[24]A. Lejeune, G. Bourgeois, and S. Mazouffre, Phys. Plasmas **19**, 073501 (2012).
[25]J. Vaudolon, B. Khiar, and S. Mazouffre, Plasma Sources Sci. Technol. **23**, 022002 (2014).
[26]M. Touzeau, M. Prioul, S. Roche, N. Gascon, C. Pérot, F. Darnon, S. Béchu, C. Philippe-Kadlec, L. Magne, P. Lasgorceix *et al.*, Plasma Phys. Controlled Fusion **42**, B323 (2000).
[27]S. Mazouffre, G. Bourgeois, L. Garrigues, and E. Pawelec, J Phys. D: Appl. Phys. **44**, 105203 (2011).
[28]W. A. Hargus, in *Proceedings of the 41st AIAA/ASME/SAE/ASEE Joint Propulsion Conference & Exhibit* (Tucson, Arizona, USA, 2005), AIAA 2005-4400.